

# 1 **Probability-based approaches for identifying low-titer antibody responses**

## 2 **against SARS-CoV-2**

3  
4 Xaquín Castro Dopico<sup>1#</sup>, Leo Hanke<sup>1°</sup>, Daniel J. Sheward<sup>1°</sup>, Sandra Muschiol<sup>2</sup>, Soo Aleman<sup>3</sup>,  
5 Nastasiya F. Grinberg<sup>4</sup>, Monika Adori<sup>1</sup>, Murray Christian<sup>1</sup>, Laura Perez Vidakovics<sup>1</sup>, Changil  
6 Kim<sup>1</sup>, Sharesta Khoenkhoen<sup>1</sup>, Pradeepa Pushparaj<sup>1</sup>, Ainhua Moliner Morro<sup>1</sup>, Marco  
7 Mandolesi<sup>1</sup>, Marcus Ahl<sup>3</sup>, Mattias Forsell<sup>5</sup>, Jonathan Coquet<sup>1</sup>, Martin Corcoran<sup>1</sup>, Joanna  
8 Rorbach<sup>6,7</sup>, Joakim Dillner<sup>8</sup>, Gordana Bogdanovic<sup>2</sup>, Gerald M. McInerney<sup>1</sup>, Tobias Allander<sup>1,2</sup>,  
9 Ben Murrell<sup>1</sup>, Chris Wallace<sup>4,9</sup>, Jan Albert<sup>1,2</sup>, Gunilla B. Karlsson Hedestam<sup>1#</sup>

10

11 Affiliations:

12 <sup>1</sup>Department of Microbiology, Tumor and Cell Biology, Karolinska Institutet, Stockholm 171 77,  
13 Sweden

14 <sup>2</sup>Department of Clinical Microbiology, Karolinska University Hospital, Stockholm 171 76, Sweden

15 <sup>3</sup>Department of Infectious Diseases, Karolinska Universitetssjukhuset, Huddinge 141 52, Sweden

16 <sup>4</sup>Cambridge Institute of Therapeutic Immunology & Infectious Disease (CITIID), Jeffrey Cheah  
17 Biomedical Centre, Cambridge Biomedical Campus, University of Cambridge, Cambridge, CB2 0AW

18 <sup>5</sup>Department of Clinical Microbiology, Umeå Universitet, Umeå 901 85, Sweden

19 <sup>6</sup>Department of Molecular Biochemistry & Biophysics, Karolinska Institutet, Stockholm 171 77,  
20 Sweden

21 <sup>7</sup>Max Planck Institute-Biology of Ageing, Karolinska Institutet Laboratory, Stockholm 171 77, Sweden

22 <sup>8</sup>Department of Laboratory Medicine, Division of Pathology, Karolinska Institutet, Huddinge 141 52,  
23 Sweden

24 <sup>9</sup>MRC Biostatistics Unit, University of Cambridge CB2 0SR, United Kingdom

25

26 <sup>°</sup>Equal contribution

27 #Correspondence

28

29

30

31 **Abstract**

32

33 The levels of the antibody response against SARS-CoV-2 varies widely between individuals,  
34 which together with the decline of antibody responses over time, complicates the correct  
35 classification of seropositivity using conventional assay cut-offs. All subjects in a cohort of  
36 SARS-CoV-2 PCR+ individuals representing different disease severity categories ( $n=105$ ), and  
37 a group of PCR+ hospital staff ( $n=33$ ), developed IgG against pre-fusion-stabilized spike (S)  
38 trimers and 97% did against the receptor-binding domain (RBD). The levels differed by several  
39 orders of magnitude and associated with disease phenotype. Concomitant analysis of a cohort  
40 of healthy blood donors and pregnant women ( $n=1,000$ ), representing individuals who had  
41 undergone milder infections, demonstrated highly variable IgG titers, including several that  
42 scored between the classical 3SD and 6SD cut-offs. Since the correct classification of  
43 seropositivity is critical for epidemiological estimates, we trained probabilistic algorithms to  
44 assign likelihood of past infection using anti-S and -RBD IgG data from PCR+ individuals and  
45 a large cohort of historical negative controls ( $n=595$ ). Applied to blood donors and pregnant  
46 women, this probabilistic approach provided a more accurate way to interpret antibody titers  
47 spread over a large continuum offering a probability-based diagnosis. The methods described  
48 here are directly applicable to serological measurements following natural infection and  
49 vaccination.

50

51

## 52 Introduction

53

54 The characterization of nascent SARS-CoV-2-specific antibody responses is critical to our  
55 understanding of the infection at both individual and population levels<sup>1</sup>. While several studies  
56 have reported antibody phenotypes of SARS-CoV-2 infection, consensus on several key issues  
57 remains outstanding, such as whether all persons who have had the infection develop antibody  
58 responses to the virus, what the duration of these responses are following peak responses and  
59 what levels provide protective immunity against re-infection<sup>2-6</sup>.

60

61 Because serological studies have such a central role, both in immunosurveillance and for our  
62 basic understanding of how humans respond to infection, there is a pressing need for robust  
63 and reproducible platforms - and statistical tools - to examine antibody titers of varying levels,  
64 as highlighted by the current SARS CoV-2 pandemic<sup>7</sup>. Antibody responses to the virus spike  
65 glycoprotein are particularly relevant as spike-directed specificities mediate virus neutralizing  
66 activity. The great majority of COVID-19 vaccines are based on the spike surface antigen as  
67 the goal is to induce neutralizing antibodies that block virus entry into Ace2-positive target  
68 cells<sup>8,9</sup>. There is, therefore, a great need for well-validated assays to monitor both infection and  
69 immunization-induced antibody responses against SARS-CoV-2 spike, and this will increase  
70 further as different spike-based vaccines are introduced world-wide and follow-up studies are  
71 undertaken to understand the magnitude and quality of responses in different target groups.

72

73 To meet this need, we developed highly sensitive and specific IgM, IgG and IgA ELISAs based  
74 on mammalian cell-expressed pre-fusion-stabilized soluble trimers of the SARS-CoV-2 spike  
75 (S) glycoprotein and the receptor-binding domain (RBD), and used them in tandem to survey  
76 serum samples from large cohort of individuals PCR+ for SARS-CoV-2. For a robust  
77 validation of the assays, we used a large set of serum samples from historical blood donors as  
78 negative controls ( $n=595$ ), which is critical for determining the assay background. We then  
79 applied these assays to blood donors and pregnant women for whom serostatus was unknown.

80

81 As we show, and as has been reported by others<sup>3,10</sup>, the magnitude of response varied greatly  
82 between individuals and was associated with disease severity. Those with most pronounced  
83 symptoms, as observed in our cohort of hospitalized patients, tended to have very high anti-  
84 viral antibody titers, while those with asymptomatic or mild disease, represented by randomly  
85 sampled blood donors and pregnant women, exhibited a range of antibody levels, some of

86 which were high and others that were close to the negative control serum samples, complicating  
87 their correct classification.

88

89 To improve upon the dichotomization of a continuous variable – which is common to many  
90 clinical tests but generally results in a loss of information<sup>11,12</sup> – we used tandem anti-S and  
91 RBD IgG data from confirmed infections and negative controls to train different probabilistic  
92 approaches to identify likelihood of past infection. Compared to strictly thresholding the assay  
93 based on standard 3SD or 6SD cut-offs, the more quantitative approaches modelled the  
94 probability a sample was positive from training responses, improving the identification of low  
95 titer values.

96

## 97 **Results**

98

99 Study samples are detailed in Table 1.

100

### 101 Antibody test development

102

103 We developed ELISA protocols to profile IgM, IgG and IgA specific for a pre-fusion  
104 conformation stabilized spike (S) glycoprotein trimer<sup>13</sup>, the RBD, and the viral nucleocapsid  
105 (N). Trimer conformation was confirmed in each batch by cryo-EM<sup>14</sup> and a representative  
106 subset of study samples was used for assay development (Fig. S1A). No reproducible IgG  
107 reactivity to S or RBD was observed across all 595 historical controls in the study, although  
108 two individuals who were PCR-positive for endemic coronaviruses (ECV+) in the last six  
109 months displayed robust IgM reactivity to both SARS-CoV-2 N and S, and two 2019 blood  
110 donors (from  $n=72$  tested) had low anti-S IgM reactivity (Fig. S1B). Thus, further investigation  
111 is required to establish the contribution of potential cross-reactive memory SARS-CoV-2  
112 responses<sup>15</sup>.

113

114 Our assay revealed a greater than 1,000-fold difference in anti-viral IgG titers between Ab-  
115 positive individuals when examining serially diluted sera, a wide range difficult to capture in a  
116 single test (Fig. S1C). In SARS-CoV-2 PCR+ individuals, anti-viral IgG titers were  
117 comparable for S ( $EC_{50}=3,064$ ; 95% CI [1,197 - 3,626]) and N ( $EC_{50}=2,945$ ; 95% CI [543 -  
118 3,936]) and lower for RBD [ $EC_{50}=1,751$ ; 95% CI 966 - 1,595]. A subset (*ca.* 10%) of the  
119 SARS-CoV-2-confirmed individuals did not have detectable IgG responses against the SARS

120 CoV-2 nucleocapsid protein (N) (Fig. S1C), as previously reported<sup>16</sup>. Therefore, we did not  
121 explore responses to N further.

122

123 Elevated anti-viral Ab titers and neutralizing responses are associated with increased disease  
124 severity

125

126 When screening all SARS-CoV-2 PCR+ individuals from whom clinical information was  
127 available ( $n=105$ ), we detected potent IgG responses against S in 100% of participants, and  
128 against RBD in 97% of persons. IgM and IgA responses were generally weaker and more  
129 variable and also spread over a large range (Fig. 1A).

130

131 To examine this further, PCR+ individuals were classified according to their clinical status as  
132 follows: non-hospitalized; hospitalized or admitted to the intensive care unit. Serum IL-6  
133 levels, a cytokine that feeds Ab production<sup>17-20</sup>, were increased in severe disease samples (Fig.  
134 1B). Furthermore, multivariate analyses revealed increased anti-viral IgM, IgG and IgA to also  
135 be associated with disease severity, as has been reported<sup>3</sup>, although IgM was reduced in  
136 intensive care samples, compared to hospitalized patients (Fig. 1C and S1D-E, Table S1).  
137 Severe disease was most associated with virus-specific IgA, suggestive of mucosal pathology.  
138 We did not observe an association between ICU or IL-6 status and IgM levels, supporting that  
139 levels of the cytokine and IgA mark a more severe clinical course of COVID-19 (Fig. S1D).  
140 IgA anti-RBD responses were lower in non-hospitalized and hospitalized females compared to  
141 males, trending similarly for S (Table S1)<sup>10</sup>.

142

143 Across all PCR+ individuals (sampled up to two months from PCR test), anti-viral IgG levels  
144 were maintained, while IgM and IgA decreased, in agreement with their circulating  $t_{1/2}$  and  
145 viral clearance (Table S1). In longitudinal patient samples (sequential sampling of PCR+  
146 individuals in the study) where we observed seroconversion, IgM, IgG and IgA peaked with  
147 similar kinetics when all three isotypes developed, although IgA was not always generated in  
148 non-hospitalized or hospitalized individuals (Fig 1D), supporting a more diverse antibody  
149 response in severe disease.

150

151 To extend these observations, we characterized the virus neutralizing Ab response in PCR+  
152 patients. Using a robust *in vitro* pseudotype virus neutralization assay<sup>21</sup>, we detected  
153 neutralizing antibodies in the serum of all SARS-CoV-2 PCR+ individuals (from  $n=48$ ).

154 Neutralizing responses were not seen in samples before seroconversion (Fig. 1D) or negative  
155 controls. A large range of neutralizing ID<sub>50</sub> titers was apparent, with binding and neutralization  
156 being highly correlated (Fig. S1D). In agreement with the binding data, the strongest  
157 neutralizing responses were observed in samples from patients in intensive care (g.mean  
158 ID<sub>50</sub>=5,058; 95% CI [2,422 - 10,564]) (Fig 1E).

159

160 In healthy blood donors and pregnant women ( $n=1,000$  collected between weeks 17-21, 2020),  
161 who did not have signs or symptoms of COVID-19 when they were sampled or two weeks  
162 prior to sampling, and had no history of being hospitalized for COVID-19, IgG titers varied  
163 greatly but were generally lower than hospitalized COVID-19 patients (Fig. 1F).

164

### 165 Probabilistic analyses of positivity

166

167 As SARS-CoV-2 results in asymptomatic or mild disease in the majority of cases, and antibody  
168 titers decline following peak responses, the detection of low titer values is critical to individual  
169 and population-level estimates of antibody-positivity. Indeed, many healthy donor test samples  
170 screen in this study had optical densities between the 3 and 6 SD cut-offs for both or a single  
171 antigen (Fig. 1E), highlighting the problem of assigning case to *low responder* values.

172

173 To improve our understanding of the assay boundary, we repeatedly analyzed a large number  
174 of historical (SARS-CoV-2-negative) controls (blood donors from the spring of 2019,  $n=595$ )  
175 alongside test samples throughout the study (Fig. 2A). We considered the spread of known  
176 negative values critical, since the use of a small and unrepresentative set of controls can lead  
177 to an incorrectly set threshold, which skews the seropositivity estimate. This is illustrated by  
178 the random sub-sampling of non-overlapping groups of negative controls, resulting in a 40%  
179 difference in the positivity estimate (Fig. 2B).

180

181 To exploit individual titers and further improve our statistical estimates, we used anti-S and  
182 RBD data from PCR+ individuals and negative controls to train probabilistic algorithms to  
183 assign likelihood of past infection. A small cohort of PCR+ individuals among Karolinska  
184 University Hospital staff ( $n=33$ ) provided additional training values four months post-PCR  
185 test.

186

187 To this end, we compared different probabilistic algorithms – namely, logistic regression  
188 (LOG), linear discriminant analysis (LDA), linear support vector machines (SVM) and  
189 quadratic SVM (SVM2) – suited to ELISA data (Fig. 2C, Materials and Methods). Using ten-  
190 fold cross validation and training models on both proteins simultaneously (S and RBD), we  
191 found all methods worked well, with sensitivity >98% and specificity >99.6% (Fig. 2D). On  
192 this metric, LDA gave the highest specificity. Logistic regression had similarly high specificity  
193 on some folds of the training data, but with higher sensitivity. We deliberately considered  
194 balanced and unbalanced folds (where case:control ratios varied between folds) and found  
195 LOG showed the least consistency across strategies, which reflects that the proportion of cases  
196 in a sample directly informs a logistic model’s estimated parameters. SVM methods had lower  
197 specificity than LDA in the training data, but higher sensitivity.

198

199 The standard methods, calling positives by a fixed number of SD above the mean of negative  
200 controls, displayed two extreme behaviors: 3-SD had the highest sensitivity (100%) while 6-  
201 SD had the highest specificity, and the lowest sensitivity (Fig. 2D), emphasizing that the  
202 number of SD above the mean is a key parameter, but one which is not learnt in any formal  
203 data-driven manner. Both SVM and LDA offer linear classification boundaries, but we can see  
204 that the probability transition from negative to positive cases is much sharper for LDA (Fig.  
205 2C) – potentially resulting in false negatives when applied to the test data, but giving the model  
206 high specificity in the training data under cross-validation. SVM exhibits a softer probability  
207 transition around its classification boundary, offering a much more nuanced approach to the  
208 points lying in the mid-range of the two proteins. SVM2 creates a nonlinear boundary, but the  
209 cross validation suggested that this didn’t improve performance relative to linear SVM.

210

211 We chose to create ensemble learners, which were an unweighted average of SVM (linear) or  
212 SVM2 (quadratic) and LDA (*ENS* and *ENS2*, respectively), as well as a LOG-LDA learner, to  
213 balance the benefits of each approach. The ensemble learners seemed to combine the benefits  
214 of their parent methods (Fig. 2C). Test data points in the lower right region of each plot are the  
215 hardest to classify due to the relative scarcity of observations in this region in the training  
216 dataset and *ENS* (SVM-LDA) showed the greatest uncertainty in these regions, appropriately.  
217 Given these results, we chose to use *ENS* (SVM-LDA), with an average sensitivity >99.1% and  
218 specificity >99.8%, to analyze the test data.

219



220 When applied to serology data, the output of *ENS* is the probability of each sample being  
221 antibody-positive. In healthy donor test data, the *ENS* learner (considering S and RBD  
222 responses in an individual sample) estimated 7.8% (95% CI [4.8-12.5]) positivity in samples  
223 collected in week 21 of 2020 (Fig. 2E, Table S2). This is in contrast to the SD thresholding,  
224 which identified 12% and 10% positivity for S and RBD, respectively at 3 SD, and 8% and 7.5,  
225 respectively at 6 SD at this time point (Table S2). Therefore, apart from providing more  
226 accurate population-level estimates, critical to seroprevalence studies, these approaches have  
227 the potential to provide more nuanced information about titers to an individual after an antibody  
228 test. For example, the test samples with a 30-60% chance of being antibody positive (Fig. 2E)  
229 can be targeted for further investigation. Moreover, such tools are applicable to other clinical  
230 metrics where a continuous scale is dichotomized and all data and code for implementation is  
231 freely available via our online repositories.

232

## 233 Discussion

234

235 Benefitting from a robust antibody test developed alongside a diagnostic clinical laboratory  
236 responsible for monitoring sero-reactivity during the pandemic, we profiled SARS-CoV-2  
237 antibody responses in three cohorts of clinical interest. COVID-19 patients receiving intensive  
238 care showed the highest anti-viral Ab titers, developing augmented serum IgA and IL-6 with  
239 worsening disease and more advance respiratory and/or gastrointestinal pathology. These  
240 results demonstrate the inflammatory nature of severe COVID-19, and support that cytokine  
241 and isotype-level measures can help patient monitoring<sup>22</sup>.

242

243 Importantly, our neutralization data illustrated that nearly all SARS-CoV-2 PCR+ individuals  
244 and healthy donors who seroconverted developed neutralizing antibodies capable of preventing  
245 S-mediated cell entry, albeit at different titers. These data support that SARS-CoV-2 infection  
246 generates a functional B cell response in the majority of people<sup>6</sup> and serve as a useful  
247 comparator to titers in response to vaccination.

248

249 Outside of the severe disease setting, it is critical to accurately determine who and how many  
250 people have seroconverted for clinical and epidemiological reasons. However, this is  
251 complicated by low titer values, which in some cases – and increasingly with time since  
252 exposure and in mild disease<sup>23,24</sup> – overlap outlier values among negative control samples. Test  
253 samples with true low anti-viral titers fall into this range, highlighting the need to better



254 understand the assay boundary. To improve upon strictly thresholding the assay, we developed  
255 probabilistic approaches that characterized uncertainty in individual measures. These and  
256 related approaches provide more statistically sound measurements at the level of cohorts and  
257 the potential to communicate more nuanced information to individual patients - although the  
258 communication of probability needs to be approached with care to ensure what is described  
259 matches what an individual interprets. Furthermore, such approaches will aid longitudinal  
260 studies of the duration of immunity after SARS-CoV-2 spike-based vaccines and natural  
261 infection and facilitate the comparison of responses between different cohorts.

## 262 **Materials and methods**

263

### 264 Human samples and ethical declaration

265 Samples from PCR+ individuals and admitted COVID-19 patients ( $n=105$ ) were collected by  
266 the attending clinicians and processed through the Departments of Medicine and Clinical  
267 Microbiology at the Karolinska University Hospital. Samples were used in accordance with  
268 approval by the Swedish Ethical Review Authority (registration no. 2020-02811). All personal  
269 identifiers were pseudo-anonymized, and all clinical feature data were blinded to the  
270 researchers carrying out experiments until data generation was complete. PCR testing for  
271 SARS-CoV-2 RNA was by nasopharyngeal swab or upper respiratory tract sampling at  
272 Karolinska University Hospital. As viral RNA levels were determined using different qPCR  
273 platforms (with the same reported sensitivity and specificity) between participants, we did not  
274 analyze these alongside other features. PCR+ individuals ( $n=105$ ) were questioned about the  
275 date of symptom onset at their initial consultation and followed-up for serology during their  
276 care, up to 2 months post-diagnosis. Serum from SARS-CoV-2 PCR+ individuals was collected  
277 6-61 days post-test, with the median time from symptom onset to PCR being 5 days. In  
278 addition, longitudinal samples from 10 of these patients were collected to monitor  
279 seroconversion and isotype persistence.

280

281 Hospital workers at Karolinska University Hospital were invited to test for the presence of  
282 SARS-CoV-2 RNA in throat swabs in April 2020 and virus-specific IgG in serum in July 2020.  
283 We screened 33 PCR+ individuals to provide additional training data for ML approaches. All  
284 participants provided written informed consent. The study was approved by the National  
285 Ethical Review Agency of Sweden (2020-01620) and the work was performed accordingly.

286

287 Anonymized samples from blood donors ( $n=100/\text{week}$ ) and pregnant women ( $n=100/\text{week}$ )  
288 were randomly selected from their respective pools by the department of Clinical  
289 Microbiology, Karolinska University Hospital. No metadata, such as age or sex information  
290 were available for these samples in this study. Pregnant women were sampled as part of routine  
291 for infectious diseases screening during the first trimester of pregnancy. Blood donors ( $n=595$ )  
292 collected through the same channels a year previously were randomly selected for use as  
293 negative controls. Serum samples from individuals testing PCR+ for endemic coronaviruses,  
294 229E, HKU1, NL63, OC43 ( $n=20$ , ECV+) in the prior 2-6 months, were used as additional  
295 negative controls. The use of study samples was approved by the Swedish Ethical Review

296 Authority (registration no. 2020-01807). Stockholm County death and Swedish mortality data  
297 was sourced from the ECDC and the Swedish Public Health Agency, respectively. Study  
298 samples are defined in Table 1.

299

### 300 Serum sample processing

301 Blood samples were collected by the attending clinical team and serum isolated by the  
302 department of Clinical Microbiology. Samples were anonymized, barcoded and stored at -20°C  
303 until use. Serum samples were not heat-inactivated for ELISA protocols but were heat-  
304 inactivated at 56°C for 60 min for neutralization experiments.

305

### 306 SARS-CoV-2 antigen generation

307 The plasmid for expression of the SARS-CoV-2 prefusion-stabilized spike ectodomain with a  
308 C-terminal T4 fibrin trimerization motif was obtained from<sup>13</sup>. The plasmid was used to  
309 transiently transfect FreeStyle 293F cells using FreeStyle MAX reagent (Thermo Fisher  
310 Scientific). The ectodomain was purified from filtered supernatant on Streptactin XT resin  
311 (IBA Lifesciences), followed by size-exclusion chromatography on a Superdex 200 in 5 mM  
312 Tris pH 8, 200 mM NaCl.

313

314 The RBD domain (RVQ – QFG) of SARS-CoV-2 was cloned upstream of a Sortase A  
315 recognition site (LPETG) and a 6xHIS tag, and expressed in 293F cells as described above.  
316 RBD-HIS was purified from filtered supernatant on His-Pur Ni-NTA resin (Thermo Fisher  
317 Scientific), followed by size-exclusion chromatography on a Superdex 200. The nucleocapsid  
318 was purchased from Sino Biological.

319

### 320 Anti-SARS-CoV-2 ELISA

321 96-well ELISA plates (Nunc MaxiSorp) were coated with SARS-CoV-2 S trimers, RBD or  
322 nucleocapsid (100 µl of 1 ng/µl) in PBS overnight at 4°C. Plates were washed six times with  
323 PBS-Tween-20 (0.05%) and blocked using PBS-5% no-fat milk. Human serum samples were  
324 thawed at room temperature, diluted (1:100 unless otherwise indicated), and incubated in  
325 blocking buffer for 1h (with vortexing) before plating. Serum samples were incubated  
326 overnight at 4°C before washing, as before. Secondary HRP-conjugated anti-human antibodies  
327 were diluted in blocking buffer and incubated with samples for 1 hour at room temperature.  
328 Plates were washed a final time before development with TMB Stabilized Chromogen  
329 (Invitrogen). The reaction was stopped using 1M sulphuric acid and optical density (OD)

330 values were measured at 450 nm using an Asys Expert 96 ELISA reader (Biochrom Ltd.).  
331 Secondary antibodies (all from Southern Biotech) and dilutions used: goat anti-human IgG  
332 (2014-05) at 1:10,000; goat anti-human IgM (2020-05) at 1:1000; goat anti-human IgA (2050-  
333 05) at 1:6,000. All assays of the same antigen and isotype were developed for their fixed time  
334 and samples were randomized and run together on the same day when comparing binding  
335 between PCR+ individuals. Negative control samples were run alongside test samples in all  
336 assays and raw data were log transformed for statistical analyses.

337

### 338 *In vitro* virus neutralisation assay

339 Pseudotyped viruses were generated by the co-transfection of HEK293T cells with plasmids  
340 encoding the SARS-CoV-2 spike protein harboring an 18 amino acid truncation of the  
341 cytoplasmic tail<sup>13</sup>; a plasmid encoding firefly luciferase; a lentiviral packaging plasmid  
342 (Addgene 8455) using Lipofectamine 3000 (Invitrogen). Media was changed 12-16 hours post-  
343 transfection and pseudotyped viruses harvested at 48- and 72-hours, filtered through a 0.45 µm  
344 filter and stored at -80°C until use. Pseudotyped neutralisation assays were adapted from  
345 protocols validated to characterize the neutralization of HIV, but with the use of HEK293T-  
346 ACE2 cells. Briefly, pseudotyped viruses sufficient to generate ~100,000 RLU were incubated  
347 with serial dilutions of heat-inactivated serum for 60 min at 37°C. Approximately 15,000  
348 HEK293T-ACE2 cells were then added to each well and the plates incubated at 37°C for 48  
349 hours. Luminescence was measured using Bright-Glo (Promega) according to the  
350 manufacturer's instructions on a GM-2000 luminometer (Promega) with an integration time of  
351 0.3s. The limit of detection was at a 1:45 serum dilution.

352

### 353 IL-6 cytometric bead array

354 Serum IL-6 levels were measured in a subset of PCR+ serum samples ( $n=64$ ) using an  
355 enhanced sensitivity cytometric bead array against human IL-6 from BD Biosciences (Cat #  
356 561512). Protocols were carried out according to the manufacturer's recommendations and  
357 data acquired using a BD Celesta flow cytometer.

358

### 359 Statistical analysis of SARS-CoV-2 PCR+ data

360 All univariate comparisons were performed using non-parametric analyses (Kruskal-Wallis,  
361 stratified Mann-Whitney, hypergeometric exact tests and Spearman rank correlation), as  
362 indicated, while multivariate comparisons were performed using linear regression of log  
363 transformed measures and Wald tests. For multivariate tests, all biochemical measures (IL-6,

364 PSV ID50 neut., IgG, IgA, IgM) were log transformed to improve the symmetry of the  
365 distribution. As “days since first symptom” and “days since PCR+ test” are highly correlated,  
366 we cannot include both in any single analysis. Instead, we show results for one, then the other  
367 (Supp. Table 1).

368

#### 369 Probabilistic algorithms for classifying antibody positivity

370 Prior to analysis, each sample OD was standardized by dividing by the mean OD of “no sample  
371 controls” on that plate or other plates run on the same day. This resulted in more similar  
372 distributions for 2019 blood donor samples with 2020 blood donors and pregnant volunteers,  
373 as well as smaller coefficients of variation amongst PCR+ COVID patients for both SPIKE and  
374 RBD.

375

376 Our probabilistic learning approach consisted of evaluating different algorithms suited to  
377 ELISA data, which we compared through ten-fold cross validation (CV): logistic regression  
378 (LOG), linear discriminant analysis (LDA), support vector machines (SVM) with a linear  
379 kernel, and quadratic SVM (SVM2). Logistic regression and linear discriminant analysis both  
380 model log odds of a sample being case as a linear equation with a resulting linear decision  
381 boundary. The difference between the two methods is in how the coefficients for the linear  
382 models are estimated from the data. When applied to new data, the output of logistic regression  
383 and LDA is the probability of each new sample being a case. Support vector machines is an  
384 altogether different approach. We opted for a linear kernel, once again resulting in a linear  
385 boundary. SVM constructs a boundary that maximally separates the classes (i.e. the margin  
386 between the closest member of any class and the boundary is as wide as possible), hence points  
387 lying far away from their respective class boundaries do not play an important role in shaping  
388 it. SVM thus puts more weight on points closest to the class boundary, which in our case is far  
389 from being clear. Linear SVM has one tuning parameter  $C$ , a cost, with larger values resulting  
390 in narrower margins. We tuned  $C$  on a vector of values (0.001, 0.01, 0.5, 1, 2, 5, 10) via an  
391 internal 5-fold CV with 5 repeats (with the winning parameter used for the final model for the  
392 main CV iteration). We also note that the natural output of SVM are class labels rather than  
393 class probabilities, so the latter are obtained via the method of Platt<sup>25</sup>.

394

395 We considered three strategies for cross-validation: i) random: individuals were sampled into  
396 folds at random, ii) stratified: individuals were sampled into folds at random, subject to  
397 ensuring the balance of cases:controls remained fixed and iii) unbalanced: individuals were

398 sampled into folds such that each fold was deliberately skewed to under or over-represent cases  
399 compared to the total sample. We sought a method with performance that was consistently  
400 good across all cross-validation sampling schemes, because the true proportion of cases in the  
401 test data is unknown, and we want a method that is not overly sensitive to the proportion of  
402 cases in the training data. We chose to assess performance using sensitivity and specificity, as  
403 well as consistency.

404  
405 Given the good performance of all learners (described in the results), we considered the  
406 prediction surface associated with each SVM, LDA, SVM-LDA ensemble, and the standard 3-  
407 SD, 6-SD hard decision boundaries. Note that while methods trained on both proteins can draw  
408 decision contours at any angle, SD methods are limited to vertical or horizontal lines. We can  
409 see that success, or failure, of the SD cut-offs depends on how many positive and negative  
410 cases overlap for a given measure (S or RBD) in the training sample. In the training data the  
411 two classes are nearly linearly separable when each protein is considered on its own, which  
412 explains good performance of 3-SD and 6-SD thresholds. However, the test data contain many  
413 more points in the mid-range of S-RBD, which makes hard cut-offs a problematic choice for  
414 classifying test samples.

415  
416 We trained the learners on all 733 training samples and used these to predict the probability of  
417 anti-SARS-CoV-2 antibodies in blood donors and pregnant volunteers sampled in 2020. We  
418 inferred the proportion of the sampled population with positive antibody status each week using  
419 multiple imputation. We repeatedly (1,000 times) imputed antibody status for each individual  
420 randomly according to the ensemble prediction, and then analyzed each of the 1,000 datasets  
421 in parallel, combining inference using Rubin's rules, derived for the Wilson binomial  
422 proportion confidence interval<sup>26</sup>.

423

#### 424 **Data and code availability statement**

425

426 Data generated as part of the study, along with custom code for statistical analyses, is openly  
427 available via our GitHub repository: <https://github.com/chrlswallace/elisa-paper>.

428

#### 429 **Author contributions**

430

431 GKH and XCD designed the study and wrote the manuscript with input from co-authors. JA,  
432 TA, JD, SM, GB, MA and SA provided the study serum samples and clinical information. LH,  
433 LPV, AMM, DJS, KCI, BM and GM generated SARS-CoV-2 antigens and pseudotyped  
434 viruses. MF and XCD developed the ELISA protocols and XCD generated the data. DJS and  
435 BM performed the neutralization assay. CW and NFG executed machine learning approaches  
436 and statistical analyses, with input from MCh and BM. MA, SK, PP, MM, JC, MCo and JR  
437 carried out wet lab experiments and assisted with data analysis.

438

### 439 **Acknowledgments**

440

441 We would like to thank the study participants and attending clinical teams. Secondly, we extend  
442 our thanks to Björn Reinius, Marc Panas, Julian Stark, Remy M. Muts and Darío Solis Sayago  
443 for their input and discussion. Funding for this work was provided by a Distinguished Professor  
444 grant from the Swedish Research Council (agreement 2017-00968) and NIH (agreement 400  
445 SUM1A44462-02). CW and NFG are funded by the Wellcome Trust (WT107881) and MRC  
446 (MC\_UP\_1302/5). For the purpose of Open Access, the author has applied a CC BY public  
447 copyright licence to any Author Accepted Manuscript version arising from this submission.

448

### 449 **Conflict of interest**

450

451 The study authors declare no competing interests related to the work.

452

### 453 **References**

454

- 455 1. Davis, M. M. A Prescription for Human Immunology. *Immunity* vol. 29 835–838  
456 (2008).
- 457 2. Sekine, T. *et al.* Robust T Cell Immunity in Convalescent Individuals with  
458 Asymptomatic or Mild COVID-19. *Cell* (2020) doi:10.1016/j.cell.2020.08.017.
- 459 3. Cervia, C. *et al.* Systemic and mucosal antibody responses specific to SARS-CoV-2  
460 during mild versus severe COVID-19. *J. Allergy Clin. Immunol.* (2020)  
461 doi:10.1016/j.jaci.2020.10.040.
- 462 4. Robbiani, D. F. *et al.* Convergent Antibody Responses to SARS-CoV-2 Infection in  
463 Convalescent Individuals. *Nature* (2020) doi:10.1101/2020.05.13.092619.
- 464 5. Dan, J. M. *et al.* Immunological memory to SARS-CoV-2 assessed for greater than



- 465 eight months after infection. *bioRxiv* (2020).
- 466 6. Gudbjartsson, D. F. *et al.* Spread of SARS-CoV-2 in the Icelandic Population. *N. Engl.*  
467 *J. Med.* (2020) doi:10.1056/nejmoa2006100.
- 468 7. Özçürümez, M. K. *et al.* SARS-CoV-2 antibody testing—questions to be asked. *J.*  
469 *Allergy Clin. Immunol.* (2020) doi:10.1016/j.jaci.2020.05.020.
- 470 8. Mulligan, M. J. *et al.* Phase I/II study of COVID-19 RNA vaccine BNT162b1 in  
471 adults. *Nature* (2020) doi:10.1038/s41586-020-2639-4.
- 472 9. Jackson, L. A. *et al.* An mRNA Vaccine against SARS-CoV-2 — Preliminary Report.  
473 *N. Engl. J. Med.* (2020) doi:10.1056/nejmoa2022483.
- 474 10. Shrock, E. *et al.* Viral epitope profiling of COVID-19 patients reveals cross-reactivity  
475 and correlates of severity. *Science* (80-. ). (2020) doi:10.1126/science.abd4250.
- 476 11. Altman, D. G. & Royston, P. The cost of dichotomising continuous variables. *British*  
477 *Medical Journal* (2006) doi:10.1136/bmj.332.7549.1080.
- 478 12. MacCallum, R. C., Zhang, S., Preacher, K. J. & Rucker, D. D. On the practice of  
479 dichotomization of quantitative variables. *Psychol. Methods* (2002) doi:10.1037//1082-  
480 989x.7.1.19.
- 481 13. Wrapp, D. *et al.* Cryo-EM structure of the 2019-nCoV spike in the prefusion  
482 conformation. *Science* (80-. ). (2020) doi:10.1126/science.aax0902.
- 483 14. Hanke, L. *et al.* An alpaca nanobody neutralizes SARS-CoV-2 by blocking receptor  
484 interaction. *Nat. Commun.* (2020) doi:10.1038/s41467-020-18174-5.
- 485 15. Herzenberg, L. A. & Herzenberg, L. A. Toward a layered immune system. *Cell* (1989)  
486 doi:10.1016/0092-8674(89)90748-4.
- 487 16. Long, Q. X. *et al.* Antibody responses to SARS-CoV-2 in patients with COVID-19.  
488 *Nat. Med.* (2020) doi:10.1038/s41591-020-0897-1.
- 489 17. Eto, D. *et al.* IL-21 and IL-6 are critical for different aspects of B cell immunity and  
490 redundantly induce optimal follicular helper CD4 T cell (Tfh) differentiation. *PLoS*  
491 *One* **6**, e17739 (2011).
- 492 18. Dienz, O. *et al.* The induction of antibody production by IL-6 is indirectly mediated by  
493 IL-21 produced by CD4 + T cells. *J. Exp. Med.* (2009) doi:10.1084/jem.20081571.
- 494 19. Maeda, K., Mehta, H., Drevets, D. A. & Coggeshall, K. M. IL-6 increases B-cell IgG  
495 production in a feed-forward proinflammatory mechanism to skew hematopoiesis and  
496 elevate myeloid production. *Blood* (2010) doi:10.1182/blood-2009-07-230631.
- 497 20. Beagley, K. W. *et al.* Interleukins and IgA synthesis. Human and murine interleukin 6  
498 induce high rate IgA secretion in IgA-committed B cells. *J. Exp. Med.* (1989)

- 499 doi:10.1084/jem.169.6.2133.
- 500 21. Bartosch, B. *et al.* In vitro assay for neutralizing antibody to hepatitis C virus:  
501 Evidence for broadly conserved neutralization epitopes. *Proc. Natl. Acad. Sci. U. S. A.*  
502 (2003) doi:10.1073/pnas.2335981100.
- 503 22. Del Valle, D. M. *et al.* An inflammatory cytokine signature predicts COVID-19  
504 severity and survival. *Nat. Med.* (2020) doi:10.1038/s41591-020-1051-9.
- 505 23. Seow, J. *et al.* Longitudinal evaluation and decline of antibody responses in SARS-  
506 CoV-2 infection. *Nat. Microbiol.* (2020) doi:10.1101/2020.07.09.20148429.
- 507 24. Long, Q. X. *et al.* Clinical and immunological assessment of asymptomatic SARS-  
508 CoV-2 infections. *Nat. Med.* (2020) doi:10.1038/s41591-020-0965-6.
- 509 25. Platt, J. & others. Probabilistic outputs for support vector machines and comparisons to  
510 regularized likelihood methods. *Adv. large margin Classif.* (1999).
- 511 26. Lott, A. & Reiter, J. P. Wilson Confidence Intervals for Binomial Proportions With  
512 Multiple Imputation for Missing Data. *Am. Stat.* (2020)  
513 doi:10.1080/00031305.2018.1473796.
- 514

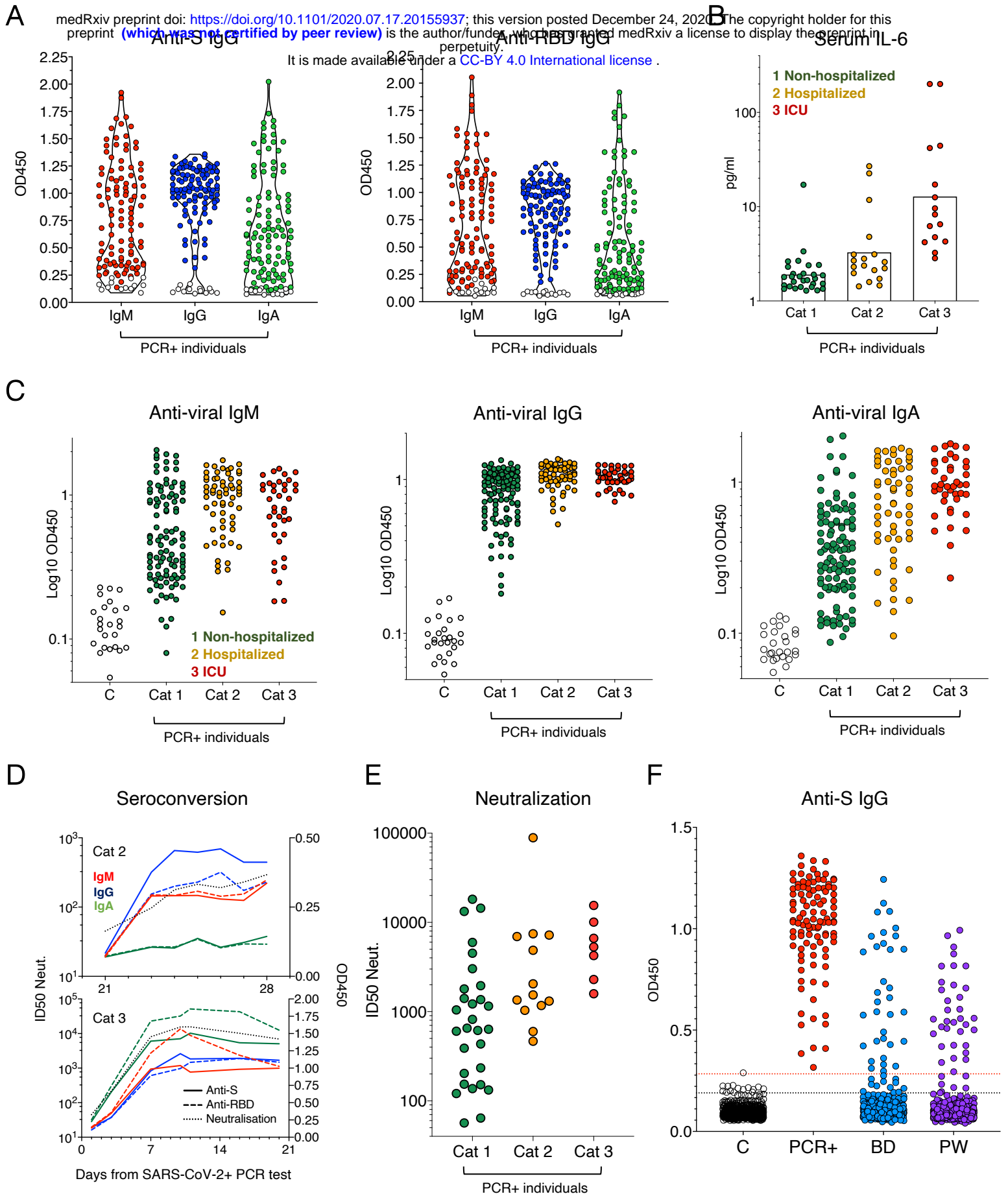
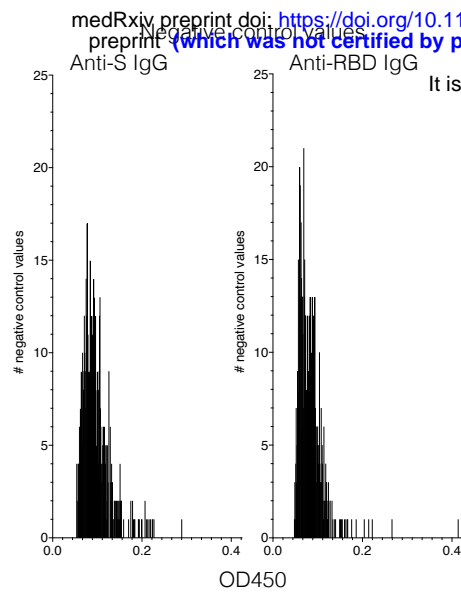


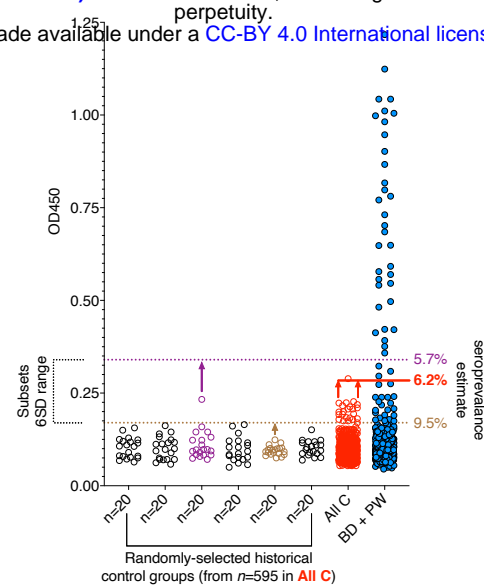
**Figure 1: Anti-SARS-CoV-2 Ab phenotypes in COVID-19 patients, PCR+ individuals, blood donors and pregnant women.**

(A) OD450nm optical density for anti-S and -RBD IgM, IgG and IgA responses in SARS-CoV-2 PCR+ individuals ( $n=105$ ), blood donors (BD,  $n=500$ ) and pregnant women (PW,  $n=500$ ). A small number of controls for each assay are represented by open circles. (B) Circulating IL-6 levels in serum are associated with disease severity. (C) Anti-viral antibody levels are associated with disease severity, most pronounced for anti-viral IgA. Anti-S and RBD responses are graphed together. (D) Two discordant longitudinal profiles of seroconversion and neutralisation capacity are shown in hospitalized COVID-19 patients. (E) *In vitro* pseudotyped virus neutralization ID<sub>50</sub> titers are associated with disease severity, with the highest titers observed in Cat 3 (ICU) patients.  $n=48$  SARS-CoV-2 PCR+ individuals were analyzed in duplicate. (F) Comparison of anti-S IgG levels between PCR+ individuals, blood donors (BD) and pregnant women (PW). 3 and 6 SD cut-offs are shown.

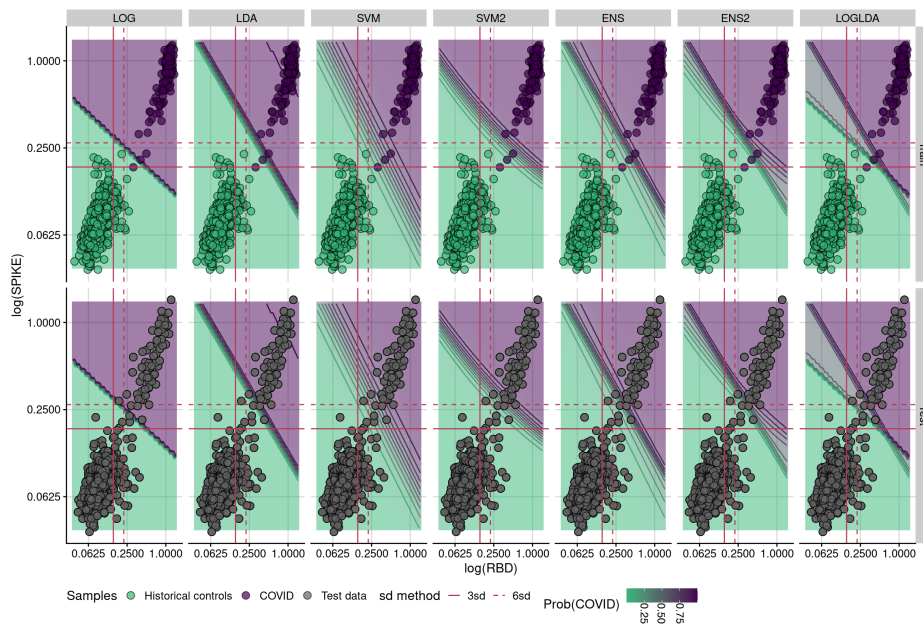
A



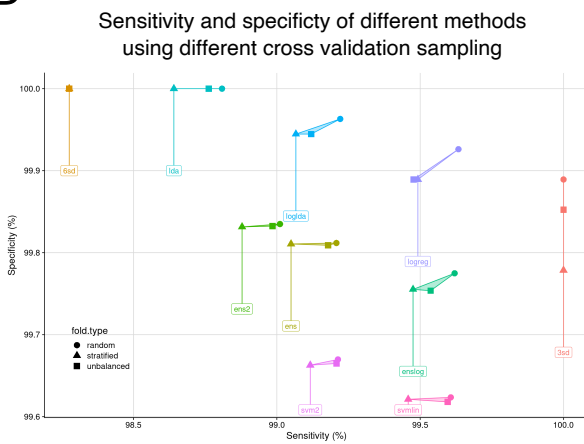
B



C



D



E

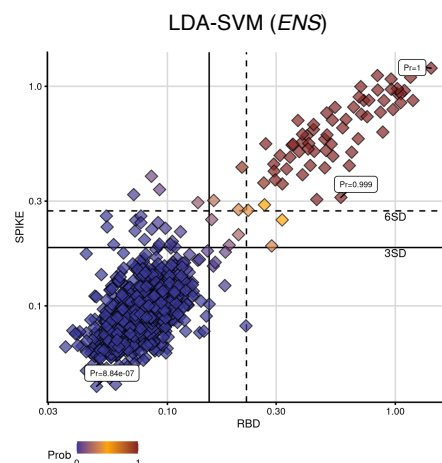


## Figure 2: Probability-based positivity estimates in blood donors and pregnant women

**(A)** Distribution of Anti-S and RBD IgG OD values for 595 historical controls (blood donors from Spring 2019). **(B)** Random sub-sampling of non-overlapping negative controls illustrates how the range of negative control (C) values can influence a conventional test cut-off, here 6 SD from the mean of the respective C groups. In the test data, depending on the control values used to set the test threshold for positivity, SP estimates vary by 40%. Blood donor and pregnant women sample values are used as an example. Anti-S IgG values are shown. **(C)** Comparison of probabilistic algorithms suited to ELISA measurements. Logistic regression (LOG), linear discriminant analysis (LDA), support vector machines (SVM) and quadratic SVM. Learners were trained using anti-S and RBD IgG data from 595 negative control values and 138 SARS-CoV-2 PCR+ individuals. Ensemble (ENS) learners were generated from the output of SVM-LDA, SVM2-LDA and LOG-LDA, as described. **(D)** Comparisons of specificity and sensitivity for the different probabilistic methods (and SD thresholding) using different cross-validation strategies. **(E)** ENS probabilities when applied to healthy donor test data, providing a highly sensitive, specific and consistent multi-dimensional solution to the problem of low responders, and assigning each data point a probability of being positive.

**Table 1 – Study samples**

<b>SARS-CoV-2 PCR+ individuals<sup>§</sup></b>	<i>n</i> =105
Females	44 (41.9%)
Males	61 (58.1%)
Median age (years)	53.0 (49-61)
Females	51.5 (48-56.2)
Males	55.0 (49-63)
Non-hospitalized ( <i>n</i> =)	53
Females, males	28, 25
Hospitalized patients ( <i>n</i> =)	31
Females, males	12, 17
Intensive care (ICU) patients ( <i>n</i> =)	21
Females, males	3, 17
SARS-CoV2+ PCR ( <i>n</i> =)	105
Sample collection dates	March-May 2020
<b>SARS-CoV-2 PCR+ KI hospital staff</b>	<i>n</i> =33
Sample collection dates	July 2020
<b>Blood donors</b>	<i>n</i> =500
Sample collection dates	Weeks 17-21 (March-August) 2020
<b>Pregnant women</b>	<i>n</i> =500
Sample collection dates	Weeks 17-21 (March-May) 2020
<b>Historical blood donors</b>	<i>n</i> =595
Sample collection dates	March-June 2019
<b>ECV+ donors</b>	<i>n</i> =20
Sample collection dates	July-December 2019

<sup>§</sup>Under the care of Karolinska University Hospital  
No additional metadata available for any samples

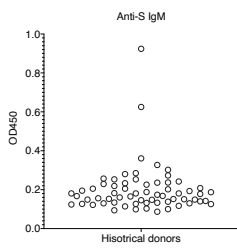
A

medRxiv preprint doi: <https://doi.org/10.1101/2020.07.17.20155937>; this version posted December 24, 2020. The copyright holder for this preprint (which was not certified by peer review) is the author/funder, who has granted medRxiv a license to display the preprint in perpetuity. It is made available under a [CC-BY 4.0 International license](https://creativecommons.org/licenses/by/4.0/).

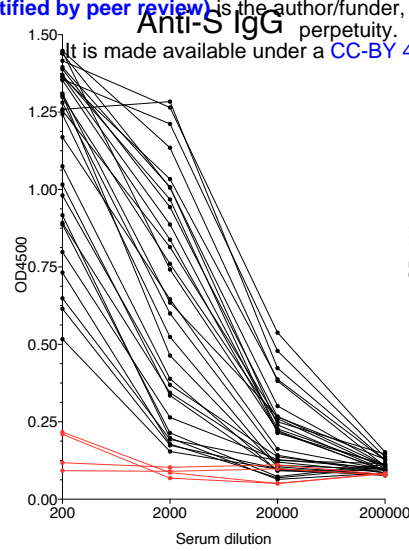
Samples used for assay development:

- 100 historical controls
- 38 PCR+ individuals
- 100 blood donor samples
- 20 individuals PCR+ for endemic coronaviruses in the past six months

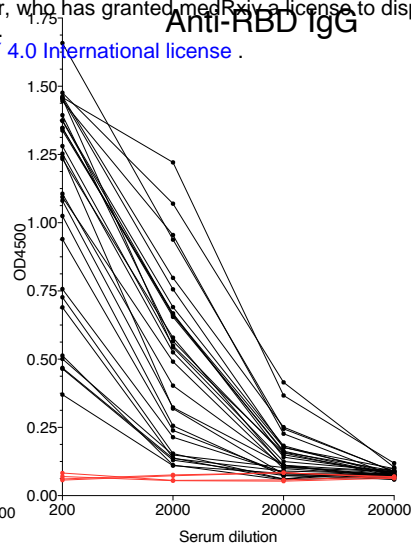
B



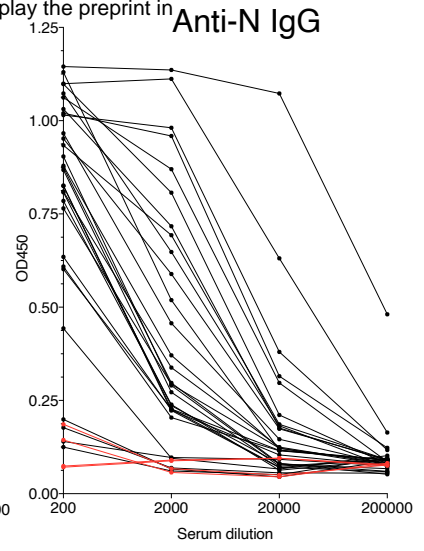
C



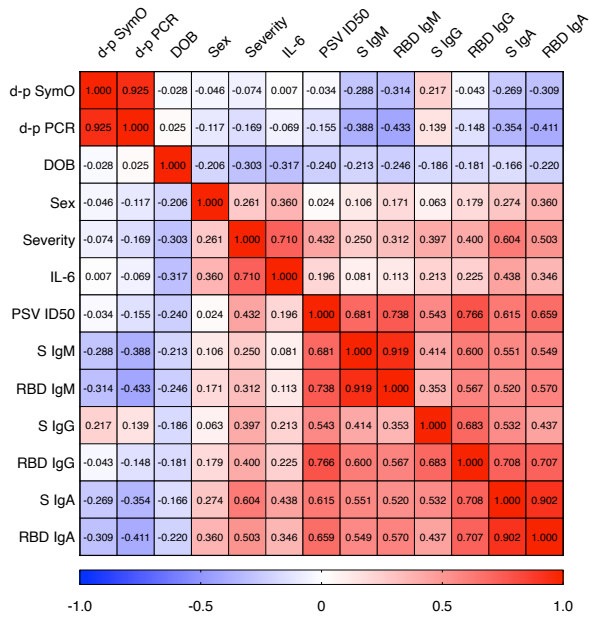
Anti-RBD IgG



Anti-N IgG



D



E

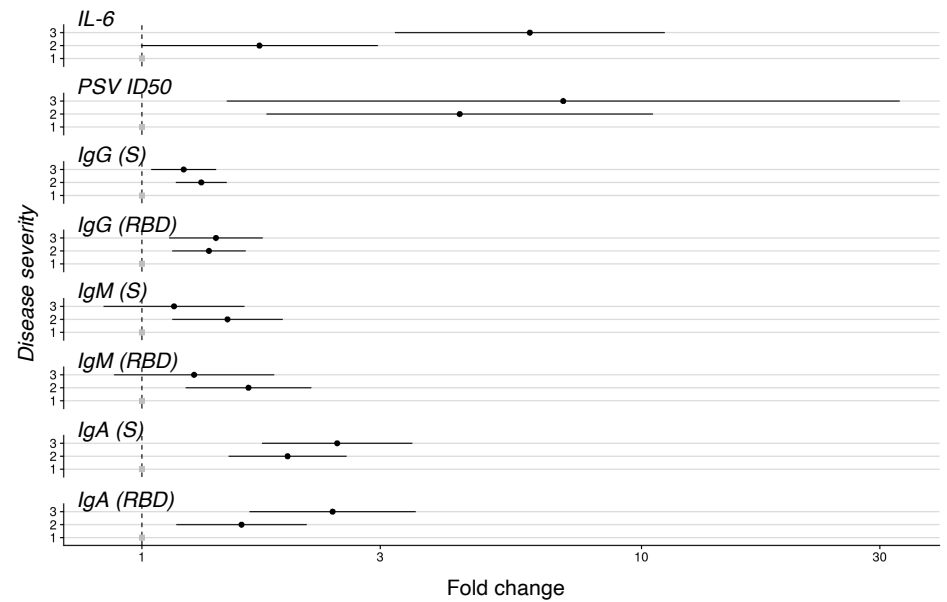


### Figure S1: Antibody phenotypes in PCR+ individuals and healthy participants

(A) Study samples used for assay development. (B) Anti-S IgM reactivity observed in a random subset of historical controls. Binding was confirmed in these samples in an independent experiment. No reproducible IgG reactivity to S trimers of the RBD was observed across all historical controls in the study. (C) Serial dilution of  $n=30$  random PCR+ individuals. ECV+ ( $n=4$ ) controls are shown in red. (D) Spearman's rank correlation of PCR+ dataset features and antibody levels. DOB - *date of birth*; d-p SymO - *days post-symptom onset*; d-p PCR - *days post SARS-CoV-2+ PCR*; PSV ID50 - *neutralizing titer*. (E) Adjusted fold-change compared to Category 1 PCR+ individuals. The effects of age (DOB), sex, days from PCR test were considered.